NUKLEONIKA 2012;57(3):357–362

ORIGINAL PAPER

Tribological effects of ion implantation of Inconel 600

Marcin Chmielewski, Marek Barlak, Katarzyna Pietrzak, Dariusz Kaliński, Ewa Kowalska, Agata Strojny-Nędza

Abstract. Commercial Inconel 600 nickel-chromium alloy was implanted with nitrogen, chromium, titanium, yttrium and copper with tin (as bronze components) ions to doses ranging from 1.6e17 to 3.5e17 cm^{-2}. The main goal of the research was to investigate the properties of the modified alloy in the context of its application in foil bearings. The virgin and the treated samples were tribologically tested and examined by scanning electron microscopy (SEM) and energy dispersive spectroscopy (EDS). The technological studies were preceded by modelling of concentration values of the introduced elements. The results obtained with the use of ion implantation are discussed.

Key words: foil bearings • ion implantation • Inconel 600 • friction coefficient

M. Chmielewski✉, K. Pietrzak, D. Kaliński, A. Strojny-Nędza
Institute of Electronic Materials Technology (IMTE), 133 Wólczyńska Str., 01-919 Warsaw, Poland,
Tel.: +48 22 835 3041 ext. 415, Fax: +48 22 834 9003,
E-mail: marcin.chmielewski@itme.edu.pl

M. Barlak, E. Kowalska
National Centre for Nuclear Research (NCBJ), 7 Andrzeja Sołtana Str., 05-400 Otwock/Świerk, Poland

Received: 17 May 2012
Accepted: 27 June 2012

Introduction

Microturbines are small devices for simultaneous production of both electricity and heat. They consist of a bearing shaft characterized by small nominal diameters (of the order of several millimetres) and an attached microturbine rotor. Microturbine rotors usually rotate fairly frequently at a speed up to 100 000 rpm and the temperature inside the microturbine is likely to reach up to several hundred degrees Celsius. One of the most crucial elements for the operation of microturbines is their bearing. Criteria for the selection of bearings include the maximum permissible rotational speed, hoisting capacity, permissible operating temperature, durability, reliability as well as repair-ease. Even a unique high rotational speed makes the application of either friction or anti-friction bearings impossible and, that is why, application of foil bearings proves to be the best solution. In the case of such bearing, a typical thick-walled bearing shell is covered with a foil set, including a bump foil and a top foil. The set of foils interacting with each other is characterized by low stiffness and good damping properties, which provides excellent conditions for its operation even at a high rotational speed. The task of the bump foil, irrespective of its shape, is to transfer the load resulting from the rotary movement of a shaft, whereas the predominant function of the top foil is to minimize the friction resistance to the rotating shaft. A schematic design of a foil bearing is presented in Fig. 1.

In industrial practice, numerous materials are used as sliding elements in foil bearings. Depending on the

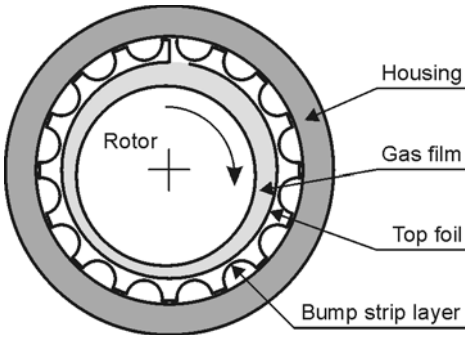

Fig. 1. Schematic design of a foil bearing.

operating conditions, pure metals, e.g. Ni, alloys based on aluminum, nickel or copper, plastic or composite materials are employed.

Foil bearings are particularly attractive for systems where conventional oil-lubricated or rolling element bearings have proved unsuitable due to temperature, rotational speed, working fluid, etc. There are numerous possible applications for foil bearings, including aircraft gas turbine engines, auxiliary power units, microturbines, pumps, compressors, cryogenic turboexpanders and turbochargers. To expand the range of their practical implementations, investigations of materials likely to satisfy many different requirements have been performed. With respect to the application as top foils both tribological properties – low friction coefficient and high wear resistance – are required.

This task can be resolved by insertion of lubricated and/or hardened element. Ion implantation is one of different methods, which can be used as the introduction of an additional element to the near surface area. This technique is widely used for modification of the surface properties of materials for different purposes, e.g. for a change of the tribological properties or improvement of the wettabillity of materials [1–3, 15, 17, 19].

There are relatively few reference data on the improvement of tribological properties of Inconel 600. One can find several examples of ion implantation in the alloys, which are chemically similar to the Inconel 600.

J. P. Rivière *et al.* [18] conducted investigations on nitrogen ion implantation ($N_2^+ + N^+$) to the AISI 316 steel and Inconel 600 alloy. The nitrogen implantation was carried out at 400°C to the substrates with average roughness of about R_a = 0.05 μm. The acceleration voltage was 1.2 kV. The current density was maintained at a level of 1 mA/cm^2. The process was performed for 1 h. These parameters correspond to the implanted dose of 3.5e19 cm^{-2}, but in connection with the sputtering, the retained dose was about 10% of the implanted dose only. For both alloys, a significant increase of hardness and the reduction of the abrasive wear was observed. The effect was connected with the formation of expanded austenite in the structure of the investigated materials.

Plasma immersion ion implantation (PI^3) method was used for the introduction of nitrogen to the substrates made of Inconel 601 alloy. The results of these investigations were described in Ref. [7]. The samples were modified for 5 h in nitrogen plasma at a constant nitrogen dose rate of 2.25e14 N/cm^{2}s at 35 kV. The sample temperature was 350 or 400°C. The observed improvement in tribological properties of investigated substrates, was also due to the formation of expanded austenite.

PI^3 method was used also in the investigations described in Ref. [14]. In this case, the substrates made of AISI P20, ASSAB 718 and AISI 420 steels were modified.

Z. Werner *et al.* [20] showed the results of copper and tin co-implantation to NC-6 steel substrates using MEVVA type accelerator. These works were aimed at a reduction of friction coefficient and an increase of the wear resistance of the modified material. The bronze cathode was used as a source of implanted ions. Due to the significant differences between sputtering coefficients of copper and tin, the maximum fluences were obtained at a level of 5.4e16 and 1.2e15 cm^{-2}, respectively.

The effect of nitrogen and titanium implantation on the tribological properties of 34S and 37HS steels was the subject of investigations described in Ref. [4]. The implanted doses were 1-6e17 and 1-5e17 cm^{-2} for N and Ti, respectively. Based on the investigation results it was found that nitrogen improves the tribological properties of steels more efficiently than titanium. It is connected with the formation of FeN phase. In the case of titanium implantation, the improvement of tribological properties is related to the formation of amorphous FeTi phase.

J. I. Oñate *et al.* [16] presented several examples of the influence of ion implantation of nitrogen, carbon, oxygen, chromium and yttrium and their combinations on the change of tribological properties of several types of steel and Ti-6Al-4V alloy. Ion energies ranged from 25 to 180 keV and the fluences from 1e17 to 7e17 cm^{-2}. According to the authors, the improvement of tribological properties of the modified materials was due to several mechanisms for strengthening the structure, such as deformation of the lattice or precipitation hardening.

In the literature, one can find descriptions of other elements used for the improvement of the tribological properties of various alloys such as iron, molybdenum, boron [6, 11, 21, 22]. The mechanisms of the structure strengthening are similar to the described above.

In this paper, we present the results of ion implantation of selected elements on the changes of tribological properties of Inconel 600 alloy.

Experimental

Modelling

The technological studies were preceded by modelling of the values of sputtering yield, the values of the maximum fluences without saturation and the profiles of the introduced elements. The modelling was performed using SUSPRE code [8].

Samples

Samples were cut from commercial nickel-chromium Inconel 600 alloy in the form of coupons of 50 × 50 × 0.1 mm^3 in size. The chemical composition of Inconel 600 (wt.%) is: min. 72.0 Ni + Co, 14.0–17.0 Cr, 6.0–10.0

Table 1. The main results of the simulation of all ion implantation processes

Ion	Projected range (nm)	Range straggling (nm)	Peak volume dopant concentrations (cm^{-2})	Sputtering yield
N	75.84	95	21.08e21	0.78
Cr	44.28	47	63.15e21	5.44
Ti	47.88	53	66.44e21	4.78
Y	30.80	28	42.95e21	10.14
Cu	36.10	36	55.46e21	7.12
Sn	19.32	17	34.29e21	12.50

Fe, max. 0.15 C, max. 1.0 Mn, max. 0.015 S, max. 0.50 Si and max. 0.50 Cu [9].

Before processing, the samples were washed in high purity acetone under ultrasonic agitation.

Processing

Copper and tin (as bronze components), titanium, chromium, yttrium and nitrogen ions were implanted into Inconel 600 coupons using an MEVVA type implanter with direct beam, without mass separation, described in detail elsewhere [5].

To avoid overheating effects, the samples were clamped onto a water-cooled stainless steel plate. In the case of the implantation of metallic ions, the ion current densities were kept below 10 $\mu A/cm^2$, so the substrate temperature did not exceed 200°C.

In the case of the implantation of nitrogen ions, the current density was in the range from 1 to 2 mA/cm^2. The sample temperature was in the range 300–400°C.

The base pressure in the vacuum chamber was about 2-5e^{-4} Pa.

Ions were implanted at 65 kV acceleration voltage. The implanted doses were 2.5e17, 3.5e17, 3.0e17, 1.6e17 and 2.2e17 cm^{-2} for Cu and Sn, Ti, Cr, Y and N, respectively. These are the values of the fluences without the saturation of the profiles, as determined by SUSPRE code. Table 1 shows the main results of the simulation for all ion implantation processes.

The implantation dose of N is relatively low. In this case, we intended to check the influence of the beam current value higher by a factor of about 100–200 in comparison to the remaining cases on the ion implantation results.

Nitrogen of 99.9% purity was used as the working gas and as the source of gaseous ions.

Characterization

The quality of the surfaces of the virgin, implanted and tribologically tested samples, were examined with the use of scanning electron microscopy (SEM) in the "compo" (composition) and "topo" (topography) mode. Also, the width of the sliding tracks was determined by the SEM method. The magnification of the observation was 80× and 400×.

The presence of the elements in the surface of the sample and in the sliding tracks was verified by energy dispersive spectroscopy method (EDS).

Tribological tests were conducted according to the following procedure. The samples were pressed against a stainless steel ball of 6.5 mm diameter with a force of F_n = 10 N. A holder together with a ball attached to it were set in reciprocating motion driven by an electrodynamic generator. The two components between which friction appeared slid on one another at a velocity of 5 mm/s. The friction force F_t then generated was measured with a piezoelectric displacement sensor at a rate of 24 cps. It was induced and recorded in the friction processes of varying length (5.0 min, 15.0 min and 30.0 min). The friction coefficient was analyzed using a special software.

The value of the roughness of the investigated samples (before and after ion implantation process) and the profiles of the sliding tracks were determined by a mechanical roughness measuring device.

Results and discussions

The average value of the roughness of the virgin samples R_a was about 0.09 μm. Practically, this value was the same after ion implantation process for all treated samples. Also, the morphology of the modified samples (not shown here) did not change during the modification process.

Figure 2 shows the results of SEM observation of the character of the typical sliding tracks for all ion

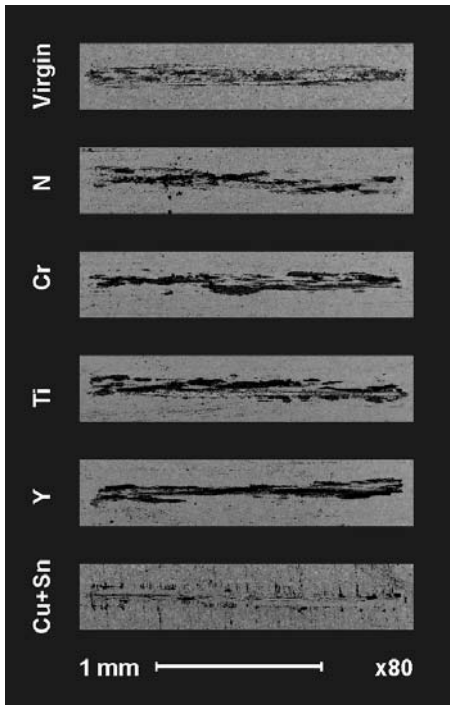

Fig. 2. The results of SEM observations (in "compo" mode) of the sliding tracks on the surface of the modified samples of Inconel 600.

modified samples. These observations were conducted at magnifications 80×, in "compo" mode. More details in the morphology of each sliding track can be seen in Fig. 3. For better visualization, SEM observation results obtained with magnification 400× in "compo" mode were compared with the results obtained in "topo" mode. In all cases, the wear track is not a classical groove after the tribological tests. The morphology of all tracks exhibits grooves parallel to the sliding direction. Additionally, in the case of: virgin, N, Cr and Ti ion implanted samples, the particles of the removed material embedded into substrates are observed. A lot of these particles is observed particularly in the virgin and N-modified samples. The sliding tracks on the Y and Cu + Sn implanted samples have different character and practically only parallel grooves are visible.

This morphology of the investigated samples indicates the typical abrasive nature of the wear (which is observed when a harder material is rubbing against a softer one) in the micro-ploughing wear mode. In this case, the material is shifted to the sides of the wear groove and it is not removed from the surface [13]. Examples of this mode were described, e.g. in Refs. [12] or [10].

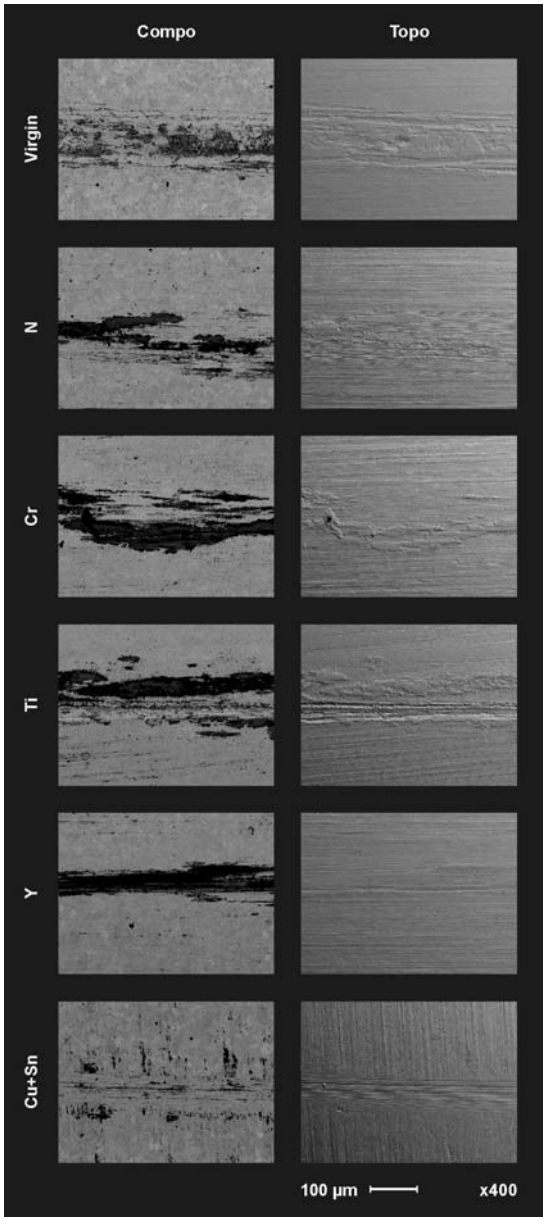

Fig. 3. The results of SEM observations (in "compo" and "topo" mode) of the sliding tracks on the surface of the modified samples of Inconel 600.

Generally, in our systems, "two body abrasive wear" is present, because there are only two rubbing components involved in the friction process. However, the presence of the embedded particles suggests the occurrence of "three body abrasive wear", which is characterized by a hard particle trapped between the rubbing surfaces. Hard particles of iron oxides could be a "third body" in our case. The EDS results (not shown here) suggest the occurrence of the process of iron oxidation in the investigated systems. This is particularly visible in the area of the embedded particles.

The appearance Fe-O phases in the system suggests additional new mechanism of the wear. Apart from the abrasive wear this is the corrosive wear mechanism [13].

Figure 4 shows the profiles of the sliding tracks. All presented profiles of the individual sliding tracks correspond exactly to the results of the microscopic

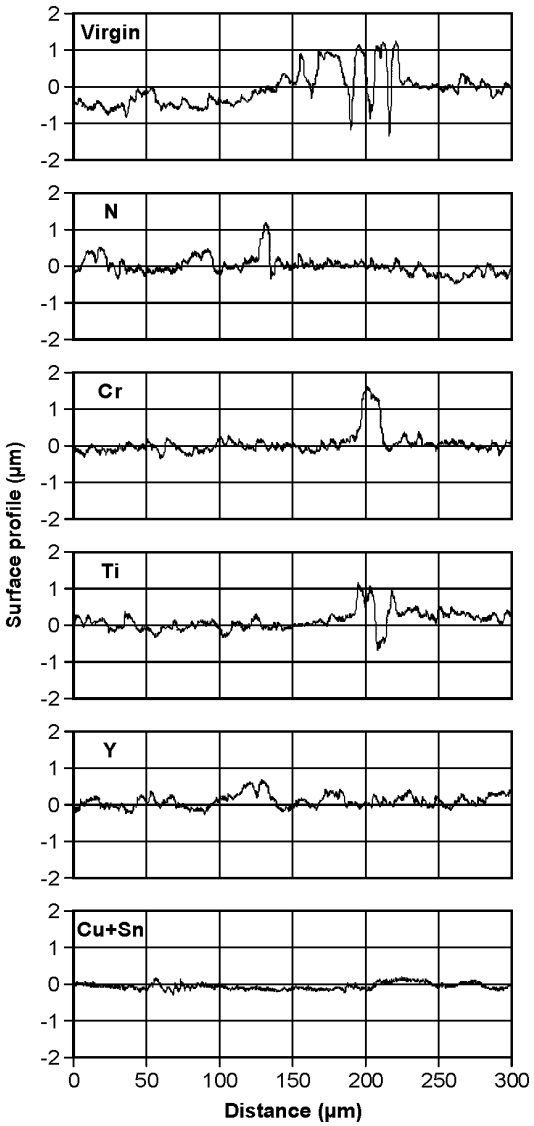

Fig. 4. The profilograms of the surfaces with the wear tracks.

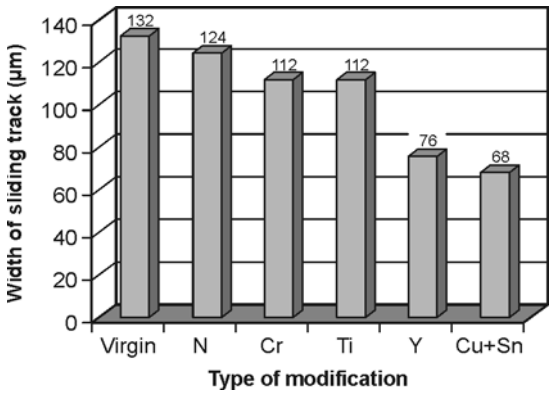

Fig. 5. The width of the sliding tracks for a virgin sample of Inconel 600 and for all types of its modification.

observations. The shape of wear tracks in virgin, N, Cr and Ti ion implanted confirm the presence of both the grooves and the embedded particles. The maximum distance between the pits and the peaks is up to about 2 μm. The surfaces of the samples modified by Y and Cu + Sn have different character. The shape of these surfaces is more smooth, without large grooves and large peaks. The surface of Cu + Sn ion implanted samples is particularly homogeneous.

Figure 5 shows the values of the width of the wear tracks for all types of the investigated samples. Each presented value is an average value determined from three measurements. The values correspond to the character of the observed wear tracks, i.e. the highest values are for virgin and N implanted samples, which were characterized by major changes in surface morphology and *vice versa* – the lowest values are for Y and Cu + Sn implanted samples, which were characterized by the smallest changes in the surface morphology. At this moment, we cannot determine whether this coincidence is accidental or substantial.

The difference between the width of the sliding tracks is over 50% in the extreme cases, i.e. between the virgin and the Cu + Sn treated samples.

The values of friction coefficient are presented in Fig. 6. These values are the average values calculated from the instantaneous values, i.e. in time of the tribological test between 200 and 1800 s (after the stabilization process). This procedure does not include the value of the friction coefficient for the virgin Inconel 600 sample. In this case, the stabilization of the value of the friction coefficient was only from 1600 s. Probably, this change of the friction coefficient of non-treated material is the result of the destruction of the surface oxide layer, which was not modified by additional elements.

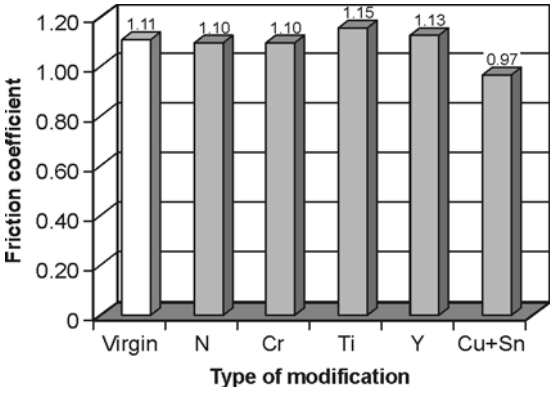

Fig. 6. The average value of the friction coefficient of Inconel 600 (between 1600 and 1800 s of the tribological test) and for all types of its modification (between 200 and 1800 s).

Conclusions

The tribological aspect of N, Cr, Ti, Y and Cu + Sn ion implantation of Inconel 600 was investigated. On the basis of the obtained results it can be concluded that:

1. Ion implantation has no influence on the roughness value and the surface morphology of the modified samples.
2. The tribological tests and EDS measurements indicate predominantly abrasive (in micro-ploughing mode) and corrosive mechanism of the wear.
3. In all cases, the wear track is not a classical groove after tribological tests. The morphology of all tracks exhibits grooves parallel to the sliding direction. The maximum distance between pits and peaks of these grooves is up to about 2 μm.
4. The values of the width of the sliding tracks correspond to the character of the observed wear tracks, but at this moment, we do not know if this is substantial or accidental coincidence.
5. The value of the friction coefficient of Cu + Sn modified samples is about 13% smaller in comparison to the virgin samples.
6. At this moment, the individual influences of Cu and Sn are unknown. This influence should be investigated in the nearest future.

Acknowledgment. The results presented in this paper have been obtained within the project "Using intelligent materials and structures to develop and implement the concept of the innovative bearing system in power microturbine rotors" (contract no. UDA-POIG.01.03.01-00-027/08-00 with the Polish Ministry of Science and Higher Education) in the framework of the Operational Programme Innovative Economy 2007–2013. The authors wish to thank Mr. J. Zagórski for technical assistance.

References

1. Barlak M, Olesińska W, Piekoszewski J *et al.* (2004) Ion implanted nanolayers in AlN for direct bonding with copper. Solid State Phenomena 99/100:231–234
2. Barlak M, Olesińska W, Piekoszewski J *et al.* (2005) Ion implantation as a pretreatment method of AlN substrate for direct bonding with copper. Vacuum 78:205–209
3. Barlak M, Piekoszewski J, Stanisławski J *et al.* (2007) The effect of titanium ion implantation into carbon ceramic on its wettability by liquid copper. Vacuum 81:1271–1274
4. Budzynski P, Youssef AA, Kamienska B (2003) Influence of nitrogen and titanium implantation on the tribological properties of steel. Vacuum 70:417–421
5. Bugaev SP, Nikolaev AG, Oks EM, Schanin PM, Yushkov GY (1994) The "TITAN" ion source. Rev Sci Instrum 65:3119–3125
6. Chen J, Conrad JR, Dodd RA (1995) Methane plasma source ion implantation (PSII) for improvement of tribological and corrosion properties. J Process Technol 49:115–124

7. Dahma KL, Short KT, Collins GA (2007) Characterisation of nitrogen-bearing surface layers on Ni-base superalloys. Wear 263:625–628
8. http://www.surrey.ac.uk/ati/ibc/research/modelling_simulation/suspre.htm
9. Inconel® alloy 600, W.Nr.2.4816, www.bibusmetals.com.pl
10. Ionescu C, Abrudeanu M, Ponthiaux P, Wenger F, Rizea V (2011) Effect of normal force on tribocorrosion behaviour of Ni-30Cr model alloy in LiOH-H_3BO_3 solution. Revue Roumaine de Chimie 56:907–915
11. Jin H, Sakai M, Wu CL, Jin JC (1997) A study of inhibitive role of Mo on the temper softening of bearing surfaces caused by ion implantation. Wear 209:193–198
12. Julián LC, Muñoz AI (2011) Influence of microstructure of HC CoCrMo biomedical alloys on the corrosion and wear behaviour in simulated body fluids. Tribol Int 44:318–329
13. Kopeliovich D, Mechanisms of wear. http://www.substech.com/dokuwiki/doku.php?id=mechanisms_of_wear
14. Lin JF, Chen KW, Xie JQ *et al*. (2002) Effects of implantation temperature and volume flow rate ratio of nitrogen and hydrogen on nitrogen concentration distribution, mechanical properties, fatigue life, fracture toughness, and tribological behavior of plasma-nitrided P20, 718 and 420 steels. Surf Coat Technol 201:5912–5924
15. Narojczyk J, Werner Z, Barlak M, Morozow D (2009) The effect of Ti preimplantation on the properties of TiN coatings on HS 6-5-2 high-speed steel. Vacuum 83:S228–S230
16. Oñate JI, Alonso F, García A (1998) Improvement of tribological properties by ion implantation. Thin Solid Films 317:471–476
17. Piekoszewski J, Kempiński W, Barlak M *et al*. (2009) Superconductivity of Mg-B layers prepared by a multi-energy implantation of boron into magnesium and magnesium into boron bulk substrates followed by the furnace and pulsed plasma annealing. Surf Coat Technol 203:2694–2699
18. Rivière JP, Méheust P, García JA, Martínez R, Sánchez R, Rodríguez R (2002) Tribological properties of Fe and Ni base alloys after low energy nitrogen bombardment. Surf Coat Technol 158/159:295–300
19. Werner Z, Barlak M, Grądzka-Dahlke M *et al*. (2007) The effect of ion implantation on the wear of Co-Cr-Mo alloy. Vacuum 81:1191–1194
20. Werner Z, Piekoszewski J, Grötzschel R, Szymczyk W (2002) Implantation of steel from MEVVA source with bronze cathode. In: Oks E, Brown I (eds) Emerging applications of vacuum-arc-produced plasma, ion and electron beams. NATO Science Series. Series II: Mathematics, Physics and Chemistry. Kluwer Academic Publishers, Dordrecht, pp 187–190
21. Yan PX, Wei ZQ, Wen XL *et al*. (2002) Post boronizing ion implantation of C45 steel. Appl Surf Sci 195:74–79
22. Zhang A, Chen J, Shi W, Liu Z (2000) Study on tribological behaviors of Fe+ ion implanted in 2024 aluminum alloy. Nucl Instrum Methods Phys Res B 169:43–47